GCK-3, a Newly Identified Ste20 Kinase, Binds To and Regulates the Activity of a Cell Cycle–dependent ClC Anion Channel

Jerod Denton,[1] Keith Nehrke,[2] Xiaoyan Yin,[1] Rebecca Morrison,[1] and Kevin Strange[1]

[1]Department of Anesthesiology, Department of Molecular Physiology and Biophysics, and Department of Pharmacology, Vanderbilt University Medical Center, Nashville, TN 37232

[2]Department of Medicine, Nephrology Unit, University of Rochester Medical Center, Rochester, NY 14642

ABSTRACT CLH-3b is a *Caenorhabditis elegans* ClC anion channel that is expressed in the worm oocyte. The channel is activated during oocyte meiotic maturation and in response to cell swelling by serine/threonine dephosphorylation events mediated by the type 1 phosphatases GLC-7α and GLC-7β. We have now identified a new member of the Ste20 kinase superfamily, GCK-3, that interacts with the CLH-3b COOH terminus via a specific binding motif. GCK-3 inhibits CLH-3b in a phosphorylation-dependent manner when the two proteins are coexpressed in HEK293 cells. *clh-3* and *gck-3* are expressed predominantly in the *C. elegans* oocyte and the fluid-secreting excretory cell. Knockdown of *gck-3* expression constitutively activates CLH-3b in nonmaturing worm oocytes. We conclude that GCK-3 functions in cell cycle– and cell volume–regulated signaling pathways that control CLH-3b activity. GCK-3 inactivates CLH-3b by phosphorylating the channel and/or associated regulatory proteins. Our studies provide new insight into physiologically relevant signaling pathways that control ClC channel activity and suggest novel mechanisms for coupling cell volume changes to cell cycle events and for coordinately regulating ion channels and transporters that control cellular Cl^- content, cell volume, and epithelial fluid secretion.

KEY WORDS: *C. elegans* • meiotic maturation • phosphorylation • oocyte • cell volume

INTRODUCTION

ClC voltage-gated Cl^- channels are present in all phyla and function in plasma and intracellular organelle membranes (Jentsch et al., 2002). The channels play key roles in diverse and fundamental physiological processes, including regulation of cytoplasmic Cl^- levels and skeletal muscle membrane excitability, transepithelial Cl^- transport, organelle acidification, regulation of nitrate content in plants, and cation homeostasis in yeast (Jentsch et al., 2002). The physiological importance of ClCs is underscored by disease-causing mutations in channel-encoding genes. Nine ClC genes have been identified in mammals, and mutations in five of these give rise to inherited muscle, bone, kidney, and neurological diseases in humans (Jentsch et al., 2002; Haug et al., 2003).

Despite intensive study and their functional importance, little is known about how ClC channels are regulated, and regulatory signaling pathways have not been defined. We recently identified a ClC-type anion channel encoded by the *clh-3* gene in *Caenorhabditis elegans* (Rutledge et al., 2001). A *clh-3* splice variant, CLH-3b, is expressed in the worm oocyte (Denton et al., 2004) and is activated during oocyte meiotic cell cycle progression, a process termed meiotic maturation, and in response to oocyte swelling (Rutledge et al., 2001, 2002; Denton et al., 2004).

CLH-3b appears to play no role in oocyte volume regulation following swelling (Rutledge et al., 2001). Induction of oocyte meiotic maturation is the physiologically relevant stimulus for channel activation (Rutledge et al., 2001). Disruption of CLH-3b expression by RNA interference or deletion mutagenesis induces premature ovulatory contractions of smooth muscle-like myoepithelial sheath cells that surround and are coupled to oocytes by gap junctions (Rutledge et al., 2001; Strange, 2002; Yin et al., 2004). Ovulatory sheath cell contraction is triggered by release of LIN-3, an EGF-like ligand, from the maturing oocyte, and subsequent activation of inositol 1,4,5-trisphosphate (IP_3)–dependent Ca^{2+} signaling pathways (Yin et al., 2004). Activation of CLH-3b depolarizes the oocyte (C. Boehmer and K. Strange, unpublished observations) and most likely the gap junction–coupled sheath cells. We have postulated that this depolarization in turn inhibits sheath cell contraction by inhibiting Ca^{2+} influx required for generating and/or maintaining IP_3-dependent release of plasma membrane Ca^{2+} from intracellular stores (Rutledge et al., 2001; Strange, 2002; Yin et al.,

Correspondence to Kevin Strange: kevin.strange@vanderbilt.edu

Abbreviations used in this paper: CHO, Chinese hamster ovary; dsRNA, double strand RNA; GCK, germinal center kinase; GST, glutathione S-transferase; HEK, human embryonic kidney; PAK, p21-activated kinase.

J. Gen. Physiol. © The Rockefeller University Press • 0022-1295/2005/02/113/13 $8.00
Volume 125 February 2005 113–125
http://www.jgp.org/cgi/doi/10.1085/jgp.200409215

2004). Regulation of sheath cell contraction by CLH-3b activity in maturing oocytes likely functions to synchronize oocyte cell cycle progression with ovulation and fertilization (Rutledge et al., 2001; Strange, 2002; Yin et al., 2004).

CLH-3b activation occurs by serine/threonine dephosphorylation mediated by the type-1 protein phosphatases GLC-7α and GLC-7β (Rutledge et al., 2002). To identify additional proteins that regulate CLH-3b activity, we performed yeast two-hybrid analysis using the intracellular COOH terminus of the channel as bait. Four interacting proteins were identified in this screen, including a member of the Ste20 (sterile 20) serine/threonine kinase superfamily. The Ste20 protein was identified originally in yeast where it functions in mitogen-activated protein kinase (MAPK) signaling cascades that control mating behavior, invasive growth, and the regulatory response to hypertonic stress (Elion, 2000; Raitt et al., 2000; Ramezani-Rad, 2003). Ste20-type kinases comprise a large superfamily that is divided into p21-activated kinase (PAK) and germinal center kinase (GCK) subfamilies (Dan et al., 2001). Members of Ste20 superfamily regulate numerous fundamental physiological processes, including the cell cycle, apoptosis, cellular stress responses, morphogenesis, and oocyte meiotic maturation (Faure et al., 1997, 1999; Cau et al., 2000; Dan et al., 2001).

The CLH-3b–interacting kinase is a newly identified member of the Ste20 superfamily and has been designated GCK-3 (germinal center kinase-3). GCK-3 is a homologue of mammalian PASK/SPAK and OSR1, and *Drosophila* Fray (Dan et al., 2001). Expression of PASK/SPAK is enriched in rat neurons and transporting epithelia (Ushiro et al., 1998). PASK/SPAK has been shown recently to bind to and regulate NKCC1, a cell shrinkage–activated Na-K-2Cl cotransporter (Piechotta et al., 2002; Dowd and Forbush, 2003).

We demonstrate here that GCK-3 binds to and functions to inhibit CLH-3b when the two proteins are coexpressed in HEK293 cells. GCK-3 inactivates CLH-3b by phosphorylating the channel and/or associated regulatory proteins. *clh-3* and *gck-3* are both expressed predominantly in the *C. elegans* oocyte and excretory cell, which functions as a secretory "epithelium" (Strange, 2003). Knockdown of *gck-3* expression by RNAi induces constitutive activation of CLH-3b in nonmaturing worm oocytes. We conclude that GCK-3 functions in cell cycle– and cell volume–regulated signaling pathways that control CLH-3b activity. Our studies provide new insights into physiologically relevant signaling pathways that control ClC channel activity and suggest novel mechanisms by which ion channels and transporters may be coordinately regulated to control cellular Cl^- content, cell volume, and transepithelial fluid secretion.

MATERIALS AND METHODS

C. elegans Strains

The wild-type Bristol N2 strain was used in this study. Worms were cultured at 16°C using standard methods (Brenner, 1974).

Yeast Two-hybrid Analysis

The bait plasmid pJP99 was created by cloning the cytoplasmic COOH terminus (amino acids 542–1001) of CLH-3b into pDBLeu (Invitrogen). pJP99 was cotransformed in the yeast strain MaV203 (genotype: *MAT*α, *leu*2-3, 112, *trp*1-901, *his*3Δ200, *ade*2-101, *gal*4Δ, *gal*80Δ, *SPAL*10::*URA*3, *GAL*1::*lacZ*, *HIS*3$_{UAS}$ *GAL*1::*HIS*3@*LYS*2, *can*1^R, *cyh*2^R) with a mixed stage *C. elegans* cDNA library (ProQuest; Invitrogen) that was ligated downstream of the GAL4 activation domain in pPC86. Approximately 0.5×10^6 yeast transformants were plated on minimal dextrose media lacking tryptophan, leucine, histidine, and uracil and containing 5 mM 3-amino triazole (MD-TLHU, 3-AT) and allowed to grow at 30°C for 1 wk. Positive clones were tested for β-galactosidase expression using a standard filter assay and then retransformed into MaV203 either alone or with pJP99. cDNA inserts of reconfirmed positive clones were sequenced. The complete mRNA sequence for the predicted gene Y59A8B.23 was determined via 5′ RACE using nested downstream gene-specific primers and an SL1 splice leader anchored upstream primer.

Quantitative liquid culture β-galactosidase assays were performed using 2-nitrophenyl β-D-galactopyranoside as a substrate (Yeast Protocols Manual; CLONTECH Laboratories, Inc.). The yeast strain AH109 (genotype: *MAT*a, *trp*1-901, *leu*2-3, 112, *ura*3-52, *his*3-200 *gal*4Δ, *gal*80Δ, *HIS*3$_{UAS}$ *GAL*1::*HIS*3@*LYS*2, *GAL*2$_{UAS}$-*GAL*2::*ADE*2, *MEL*1$_{UAS}$-MEL1::lacZ@*URA*3) was transformed with either pJP99 or pJP99(F679A) in which phenylalanine 679 of CLH-3b was mutated to alanine. Yeast were cotransformed with pPC86 as a negative control or pJP101-29, which consisted of GCK-3 (amino acids 419–596) ligated downstream of the GAL4 activation domain in pPC86. CLH-3b fusion protein expression was confirmed by Western blotting of yeast extracts with an anti-GAL4 binding domain monoclonal antibody (not depicted).

Glutathione S-Transferase Affinity Assays

A fusion protein consisting of amino acids 604–1001 of the CLH-3b COOH terminus fused to glutathione S-transferase (GST) was generated in BL21 *Escherichia coli* and immobilized on glutathione Sepharose 4B. Chinese hamster ovary (CHO) cells were cultured in Ham's F12 medium (GIBCO BRL) containing 10% FBS (Hyclone Laboratories, Inc.), 50 U/ml penicillin, and 50 μg/ml streptomycin. Cells grown in 60-mm diameter tissue culture plates to ~50% confluency were transfected using FuGENE (Roche Diagnostics Corporation) with 1.3 μg of V5-tagged GCK-3 cDNA ligated into pcDNA3.1 and grown at 37°C for 24 h. Two 60-mm plates were rinsed twice with PBS (2.7 mM KCl, 144 mM NaCl, 1.5 mM KH_2PO_4, 8.1 mM Na_2HPO_4, pH 7.4) and placed on ice. Cells were lysed by adding 0.5 ml of PBS containing 1% Triton X-100 and complete protease inhibitor cocktail (Roche Diagnostics). Lysed cells were scraped into a microcentrifuge tube, passed through a 25-gauge needle, and incubated on ice for 20–30 min. Lysates were centrifuged for 20 min at 10,000 *g* and 4°C, and pooled supernatants were incubated at room temperature with either glutathione Sepharose 4B alone or the immobilized CLH-3b GST fusion protein. After 90 min, the Sepharose was washed five times with 1 ml of PBS, resuspended in 120 μl of Laemmli buffer containing 2% SDS and 200 mM DTT, and heated to 60°C for 60 min. V5-tagged GCK-3 was identified by Western blotting using an anti-V5 antibody (Invitrogen).

Transfection and Whole Cell Patch Clamp Recording

HEK293 (human embryonic kidney) cells were cultured in 35-mm diameter tissue culture plates in Eagle's minimal essential medium (MEM; GIBCO BRL) containing 10% FBS (Hyclone), nonessential amino acids, sodium pyruvate, 50 U/ml penicillin, and 50 μg/ml streptomycin. After reaching ~50% confluency, cells were transfected using Superfect reagent (QIAGEN) with 1 or 2 μg GFP, 1 μg CLH-3b, and 1 μg GCK-3 cDNA ligated into pcDNA3 or pcDNA3.1. The total amount of cDNA transfected into cells for all experiments was 3 μg. Cells were transfected for 3 h, washed three times with MEM, and incubated overnight at 37°C.

HEK293 cells were patch clamped ~24 h after transfection. 2 h before initiating electrophysiological experiments, transfected cells were dissociated by exposure to 0.25% trypsin containing 1 mM EDTA (GIBCO BRL) for 45 s and then plated onto poly-L-lysine–coated coverslips. Plated coverslips were placed in a bath chamber mounted onto the stage of an inverted microscope. Cells were visualized by fluorescence and differential interference contrast microscopy.

Transfected cells were identified by GFP fluorescence and patch clamped using a bath solution containing 90 mM NMDG-Cl, 5 mM $MgSO_4$, 1 mM $CaCl_2$, 12 mM Hepes free acid titrated to pH 7.0 with CsOH, 8 mM Tris, 5 mM glucose, 80 mM sucrose, and 2 mM glutamine (pH 7.4, 295 mOsm), and a pipette solution containing 116 mM NMDG-Cl, 2 mM $MgSO_4$, 20 mM Hepes, 6 mM CsOH, 1 mM EGTA, 2 mM ATP, 0.5 mM GTP, and 10 mM sucrose (pH 7.2, 275 mOsm). Cells were swollen by exposure to a hypotonic (225 mOsm) bath solution that contained no added sucrose. Exposure to hypotonic solution was limited to 1 min to avoid contamination of CLH-3b current traces by activation of the ubiquitous outwardly rectifying Cl^- current $I_{Cl,swell}$ (Rutledge et al., 2002).

HEK293 were depleted of ATP by incubation for 20–30 min with 5 mM 2-deoxyglucose and 1 μM rotenone and patch clamped with an ATP-free pipette solution containing 40 μM oligomycin, 20 μM rotenone, and 5 μM iodoacetate. Metabolic inhibitors were dissolved as stock solutions in DMSO and then added to the pipette or bath saline at a final DMSO concentration of ≤0.01%.

Late-stage, meiotically arrested *C. elegans* oocytes were isolated as described previously (Rutledge et al., 2001). Oocytes were patch clamped using a bath solution containing 116 mM NMDG-Cl, 2 mM $CaCl_2$, 2 mM $MgCl_2$, 25 mM HEPES, and 71 mM sucrose (pH 7.3, 340 mOsm) and a pipette solution containing 116 mM NMDG-Cl, 2 mM $MgSO_4$, 20 mM HEPES, 6 mM CsOH, 1 mM EGTA, 48 mM sucrose, 2 mM ATP, and 0.5 mM GTP (pH 7.2, 315 mOsm). Swelling was induced by exposure to a hypotonic (260 mOsm) bath solution that contained no added sucrose.

Patch electrodes were pulled from 1.5-mm outer diameter silanized borosilicate microhematocrit tubes; electrode resistance ranged from 2 to 4 MΩ. Currents were measured with an Axopatch 200B (Axon Instruments) patch clamp amplifier. Electrical connections to the patch clamp amplifier were made using Ag/AgCl wires and 3 M KCl/agar bridges. Data acquisition and analysis were performed using pClamp 8 software (Axon Instruments).

I–V relationships were constructed from mean CLH-3b current values recorded over the last 20 ms of each test pulse. Coexpression of GCK-3 causes striking hyperpolarizing shifts in the voltage dependence of CLH-3b activation (e.g., Fig. 2). As described previously (Denton et al., 2004), we are unable to estimate the half-activation potential for CLH-3b from Boltzmann analyses of tail currents because CLH-3b inactivates too rapidly at positive potentials to reliably separate channel current from capacitance current. Hyperpolarizing test pulses also cannot be used for Boltzmann analysis because maximum channel open probability occurs at potentials more negative than −170 mV. Voltage clamping HEK293 cells beyond this voltage is difficult due to the instability of the cell membrane, particularly during swelling and metabolic poisoning experiments. We therefore estimated the channel activation voltage from *I–V* relationships. CLH-3b activates between −20 and −40 mV when expressed alone, and between −60 and −100 mV when coexpressed with GCK-3 (Fig. 2). Activation voltage was determined by fitting a straight line between −40 and −60 mV for CLH-3b alone and −80 and −100 mV for the channel expressed with GCK-3 and extrapolating back to the zero current voltage. The activation voltage was defined as the zero current intercept of this line.

Time constants for hyperpolarization-induced activation were determined by fitting current traces with mono- or bi-exponential functions over the first 500 ms of test pulses following decay of the capacitance transient. The fitting requirements for CLH-3b expressed alone or coexpressed with GCK-3 were different, making it difficult to readily compare time constants between different experimental groups and conditions. We present the time constants of activation of CLH-3b expressed in the presence and absence of GCK-3 and discuss possible functional implications. However, to simplify data presentation and interpretation, we report and compare under different experimental conditions times required to reach 50% current activation during 1-s hyperpolarizing test pulses.

RNA Interference

cDNA templates for GFP and GCK-3 (bp 1010–1810) were amplified from pPD128.110 (www.ciwemb.edu/pub/FireLabInfo/FireLabVectors) and a *C. elegans* cDNA library (provided by R. Barstead, Oklahoma Medical Research Foundation, Oklahoma City, OK). Sense and antisense RNA were synthesized by T7 polymerase (MEGAscript; Ambion) and annealed dsRNA was purified using an RNeasy Mini Kit (QIAGEN). RNA size, purity, and integrity were assayed on agarose gels. Annealed dsRNA was diluted into Tris phosphate buffer for injection. Worms were injected in one gonad arm with ~1,000,000 molecules of either GFP or GCK-3 dsRNA. Oocytes were isolated for patch clamping 20–24 h after injection.

Single Oocyte RT-PCR

Gonad arms were dissected in egg buffer as described previously (Rutledge et al., 2001), transferred through two separate 10 ml buffer washes, and then placed in a disposable 0.25-ml bath chamber. After an oocyte was ejected, the gonad was removed and the chamber perfused with 50 ml of egg buffer. Single washed oocytes were transferred by micropipette to 2 μl of distilled water in a PCR tube and lysed by freezing–thawing. Samples of perfusate surrounding oocytes were also placed into PCR tubes as a negative control. The volume transferred was approximately two- to threefold greater than the fluid volume transferred with the oocyte. RT-PCR was performed to determine the presence of GCK-3 transcripts in oocytes using the Titan One Tube RT-PCR System (Roche). The following thermocycle program was used for RT-PCR: 1x [50°, 30 min], 32x [94°, 30 s; 58°, 30 s; 68°, 1 min], 1x [68°, 7 min]. PCR primers flanked DNA sequence containing two introns in order to distinguish amplification of cDNA from genomic DNA.

Construction of Transgenes and Transgenic Worms

A GCK-3 transcriptional GFP reporter was created by PCR amplification of ~3.5 kb of genomic sequence upstream of the start

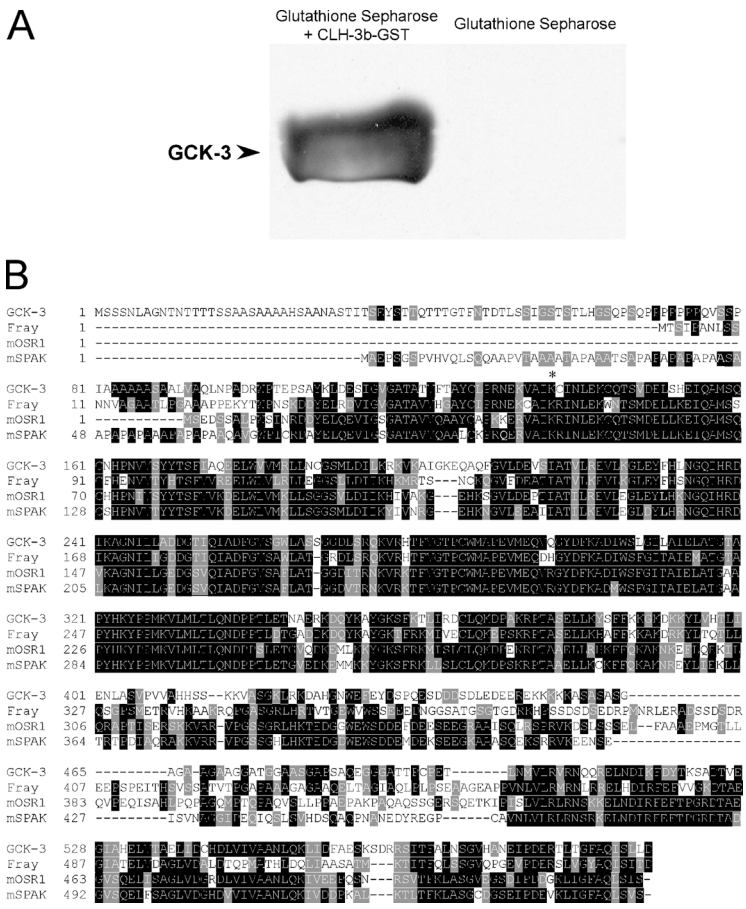

FIGURE 1. CLH-3b interacts with the Ste20 kinase GCK-3. (A) Western blot of lysates from CHO cells expressing full-length V5-tagged GCK-3. Lysates were incubated with a CLH-3b COOH terminus (amino acids 604–1001) GST fusion protein immobilized on glutathione Sepharose 4B or with glutathione Sepharose 4B alone. (B) Sequence alignment of *C. elegans* GCK-3, *Drosophila* Fray, and mouse SPAK (also known as PASK) and OSR1. Sequences were aligned using ClustalW. Identical residues and conserved substitutions are shown in black and gray, respectively. Asterisk indicates location of conserved lysine residue required for kinase activity.

codon. The PCR product was inserted into the vector pFH6.II (Nehrke and Melvin, 2002), and transgenic worms were generated by DNA microinjection as described by Mello et al. (1991) using *rol-6* as a transformation marker. Transgenic worms were imaged at room temperature by confocal microscopy using a Carl Zeiss MicroImaging, Inc. LSM510 laser scanning microscope, a Carl Zeiss MicroImaging, Inc. Plan-NeoFluar 40X/1.3 N.A. objective lens, and LSM510 imaging software. GFP was excited at 488 nm, and emission was detected through a 505–550-nm barrier filter. Differential interference contrast and fluorescence micrographs were combined using Adobe Photoshop software.

Statistical Analyses

Data are presented as means ± SEM. Statistical significance was determined using Student's two-tailed *t* test or ANOVA. P values of <0.05 were taken to indicate statistical significance.

RESULTS

GCK-3, a Novel C. elegans Ste20-Related Kinase, Interacts with the COOH Terminus of CLH-3b

To identify putative CLH-3b regulatory proteins, we performed yeast two-hybrid analysis using the channel intracellular COOH terminus (amino acids 542–1001) as bait. Of ~36 positive clones that were recovered, three coded for the COOH-terminal portion of the predicted Y59A8B.23 open reading frame. The full-length Y59A8B.23 cDNA sequence was obtained using nested 5′ RACE and found to encode a previously undescribed Ste20 superfamily kinase that has been termed germinal center kinase-3 (GCK-3; Genbank/EMBL/DDBJ accession no. AY741200).

We confirmed the interaction between CLH-3b and GCK-3 by GST affinity assay. Lysates from CHO cells expressing full-length GCK-3 tagged with a V5 epitope were incubated with a CLH-3b COOH terminus (amino acids 604–1001) GST fusion protein immobilized on glutathione Sepharose beads. As shown in Fig. 1 A, GCK-3 interacted with the CLH-3b COOH terminus fusion protein, but not with glutathione Sepharose alone.

Phylogenetic analysis indicates that GCK-3 is a homologue of mammalian PASK/SPAK and OSR1, and *Drosophila* Fray (Dan et al., 2001). A multiple sequence alignment of these four proteins is shown in Fig. 1 B.

GCK-3 Regulates Heterologously Expressed CLH-3b by Phosphorylation-dependent Mechanisms

As discussed earlier, CLH-3b is activated in vivo by serine/threonine dephosphorylation during oocyte meiotic maturation or by oocyte swelling (Rutledge et al., 2001, 2002). Given the interaction of GCK-3 and

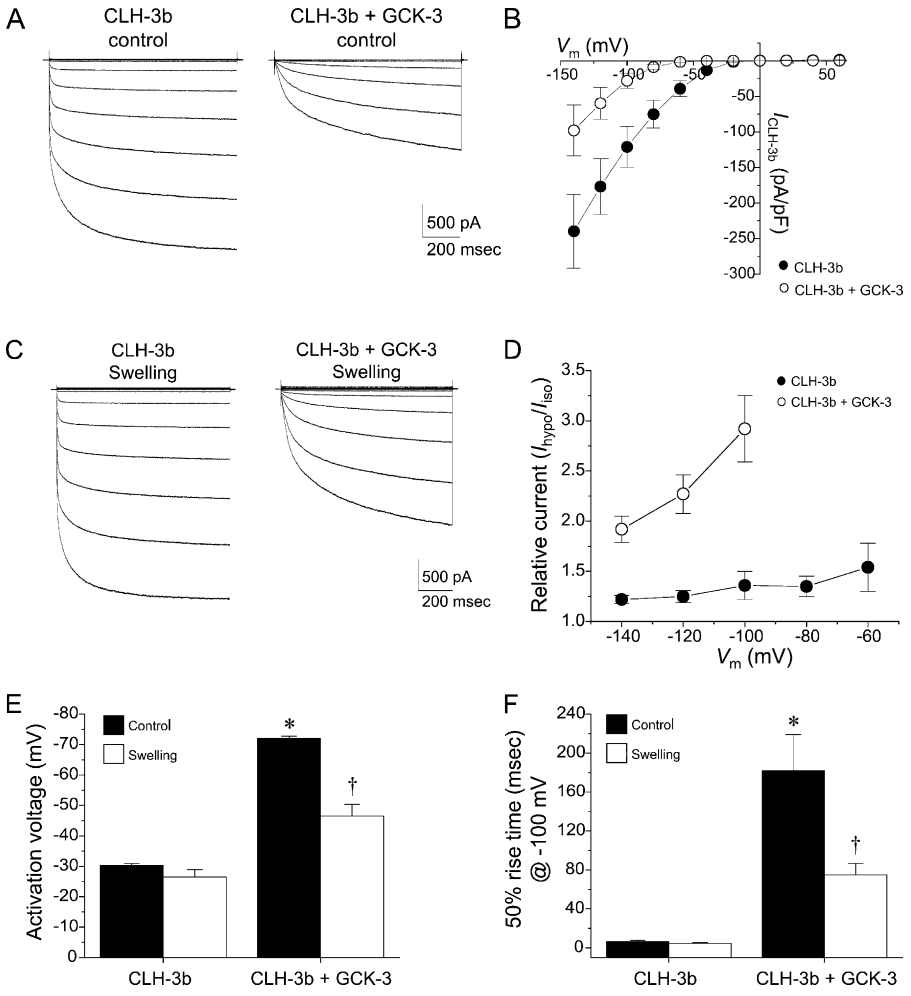

FIGURE 2. GCK-3 inhibits heterologously expressed CLH-3b. (A) Whole cell currents in HEK293 cells expressing CLH-3b alone or CLH-3b and GCK-3. Currents were evoked by stepping membrane voltage for 1 s between −140 and +60 mV in 20-mV increments from a holding potential of 0 mV. Test pulses were followed by a 1-s interval at 0 mV. Each family of current traces shown is the mean of eight cells. (B) Current-to-voltage relationships of the whole cell currents shown in A. Coexpression of CLH-3b and GCK-3 significantly ($P < 0.03$) reduces current density over the entire range of potentials where the channels were active. Values are means ± SEM ($n = 8$). (C) Mean whole-cell currents in cells expressing CLH-3b alone or together with GCK-3 after 1 min of swelling ($n = 8$ each). Data are from the same cells as shown in A. (D) Relative swelling-induced whole cell current in cells expressing CLH-3b alone or coexpressing CLH-3b and GCK-3. Cells were swollen for 1 min. Values are means ± SEM ($n = 8$). Relative current values were calculated only for test potentials where current amplitude was measurable. (E) Activation voltages and (F) 50% rise times of whole cell currents in cells expressing CLH-3b alone or coexpressing CLH-3b and GCK-3. GCK-3 decreases channel voltage sensitivity and slows hyperpolarization-induced channel activation. Cells were swollen for 1 min. Values are means ± SEM ($n = 8$). *, $P < 0.0001$ compared with cells expressing CLH-3b alone. †, $P < 0.0001$ compared with nonswollen cells.

CLH-3b, and the importance of Ste20-related serine/threonine kinases in regulating cell cycle events (Dan et al., 2001) and the yeast hypertonic stress response (Raitt et al., 2000), we tested the hypothesis that the kinase functions normally to inactivate the channel by phosphorylation.

Expression of CLH-3b in HEK293 cells generated robust hyperpolarization-evoked Cl^- currents (I_{CLH-3b}) with rapid activation kinetics and a relatively low voltage threshold for channel activation (Fig. 2, A and B). The voltage-dependent properties resemble those of native oocyte I_{CLH-3b} activated by meiotic maturation or hypotonic cell swelling (Rutledge et al., 2001, 2002; Denton et al., 2004), suggesting that CLH-3b expressed alone is constitutively active.

Coexpression of GCK-3 and CLH-3b led to striking alterations of I_{CLH-3b} functional properties. Fig. 2 A shows mean whole cell current traces recorded between −140 and 60 mV in 20-mV increments from HEK293 cells expressing CLH-3b alone or coexpressing the channel and GCK-3. Mean ± SEM current–voltage (*I–V*) relationships for these currents are shown in Fig. 2 B. GCK-3 coexpression led to three- to ninefold reductions ($P \leq 0.03$) in current density over the entire range of potentials where I_{CLH-3b} was active. The reduction in current amplitude was accompanied by a significant ($P < 0.0001$) hyperpolarizing shift in the activation voltage. CLH-3b expressed alone activated at −30 mV (Fig. 2 E, closed bars on left), whereas CLH-3b coexpressed with GCK-3 activated at −72 mV (Fig. 2 E, closed bars on right).

GCK-3 coexpression also dramatically slowed the kinetics of hyperpolarization-induced current activation (Fig. 2 A). As shown in Fig. 2 F (closed bars on left), the mean time required to reach 50% current activation (i.e., 50% rise time) in response to a 1-s step in membrane voltage from 0 to −100 mV is 7 ms when CLH-3b is expressed alone. Coexpression of CLH-3b and GCK-3

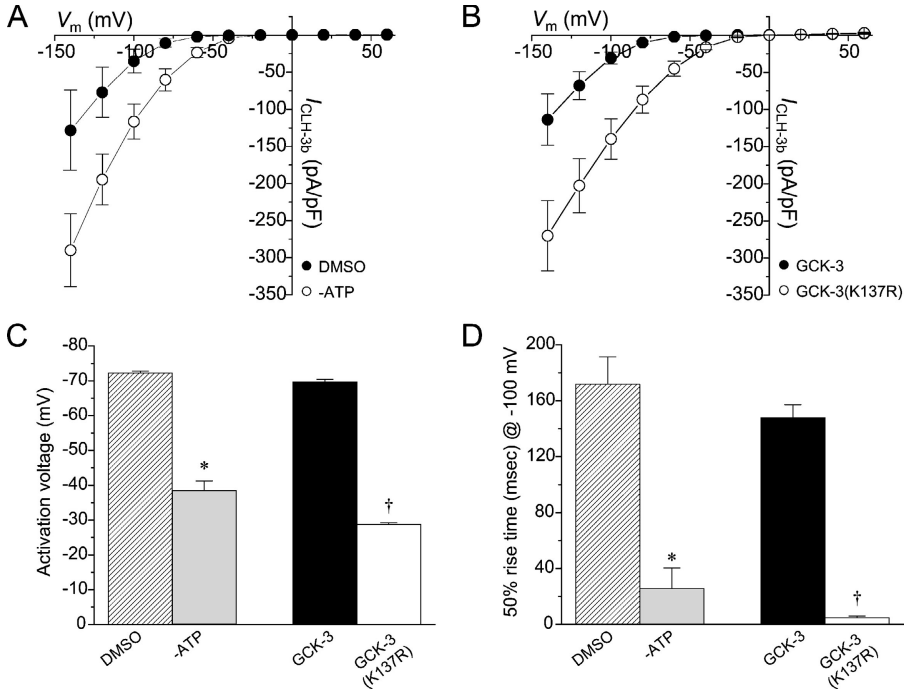

FIGURE 3. GCK-3–mediated phosphorylation regulates CLH-3b activity. (A) Current-to-voltage relationships of whole cell currents recorded from cells treated with vehicle (DMSO) or metabolic poisons and dialyzed with an ATP-free pipette solution (−ATP). ATP depletion significantly ($P < 0.04$) increases current density over the entire range of potentials where the channels were active. Values are means ± SEM (n = 7–10). (B) Current-to-voltage relationships of whole cell currents in HEK293 cells coexpressing CLH-3b and the wild-type GCK-3 or kinase-defective K137R GCK-3 mutant (GCK-3(K137R)). GCK-3(K137R) had no inhibitory effect on current density over the entire range of potentials where the channels were active. Current density in GCK-3(K137R)–expressing cells was significantly ($P < 0.04$) greater than that observed in cells expressing wild-type GCK-3. Values are means ± SEM (n = 4). Voltage clamp protocol in A and B is the same as described in Fig. 2 legend. Effect of ATP depletion and GCK-3(K137R) on whole cell current activation voltages (C) and 50% rise times (D). ATP depletion or inhibition of GCK-3 kinase activity by K137R mutation depolarized the activation voltage and decreased the rate of hyperpolarization-induced current activation. Values are means ± SEM (n = 7–10 for ATP depletion and n = 4 for kinase mutation). *, $P < 0.0001$ compared with DMSO controls. †, $P < 0.0001$ compared with wild-type GCK-3.

significantly ($P < 0.0001$) increased the 50% rise time to a mean value of 182 ms (Fig. 2 F, closed bars on right). CLH-3b activity in the *C. elegans* oocyte is low under basal conditions (Rutledge et al., 2001, 2002; Denton et al., 2004; see Fig. 6 B). The hyperpolarized activation voltage and slowed activation kinetics observed when CLH-3b is coexpressed with GCK-3 in HEK293 cells are remarkably similar to those of the *C. elegans* oocyte I_{CLH-3b} before activation by meiotic maturation or oocyte swelling (Rutledge et al., 2001; Denton et al., 2004).

CLH-3b is activated ~20-fold when *C. elegans* oocytes are swollen by exposure to a hypotonic bath solution (Rutledge et al., 2001). If GCK-3 functions normally to inactivate CLH-3b, and if it is part of the signaling pathway involved in cell volume–dependent channel regulation, then the kinase should alter swelling-induced current activation in HEK293 cells. As shown in Fig. 2 (C and D), cell swelling induced by a 1-min exposure to a 230 mOsm bath solution increased I_{CLH-3b} recorded between −140 and −60 mV by 20–50% in CLH-3b-expressing HEK293 cells. In contrast, the degree of swelling-induced current activation was five- to ninefold greater ($P < 0.0002$) in cells coexpressing GCK-3 and CLH-3b.

Swelling-induced activation of native CLH-3b is accompanied by large increases in channel voltage sensitivity and the rate of hyperpolarization-induced channel activation (Rutledge et al., 2001; Denton et al., 2004). Cell swelling had no significant ($P > 0.05$) effect on the activation voltage or kinetics of hyperpolarization-induced current activation in HEK293 cells expressing CLH-3b alone (Fig. 2, E and F, open bars on left). However, in cells coexpressing the channel and GCK-3, cell swelling significantly ($P < 0.0001$) decreased activation voltage from −72 to −47 mV and also significantly ($P < 0.04$) reduced the 50% rise time from 182 to 75 ms (Fig. 2, E and F, open bars on right). Taken together, the data in Fig. 2 demonstrate that CLH-3b expressed alone in HEK293 cells is largely constitutively active and that coexpression with GCK-3 partially inhibits the channel. Channels that have been inhibited by GCK-3 are activated dramatically by cell volume increase.

We performed two sets of experiments to determine if the GCK-3–induced inhibition of CLH-3b is mediated by phosphorylation reactions. We first tested if intracellular ATP depletion by metabolic poisoning prevents inhibition of I_{CLH-3b}. ATP depletion should inhibit GCK-3 activity and has been shown to cause constitutive activation of native I_{CLH-3b} in *C. elegans* oocytes (Rutledge et al., 2002; Denton et al., 2004). As shown in Fig. 3 A, ATP depletion increased whole cell current density 2–11-fold ($P < 0.05$) over the entire range of potentials where I_{CLH-3b} was active. In addition, ATP depletion significantly ($P < 0.0001$) reduced the activation voltage

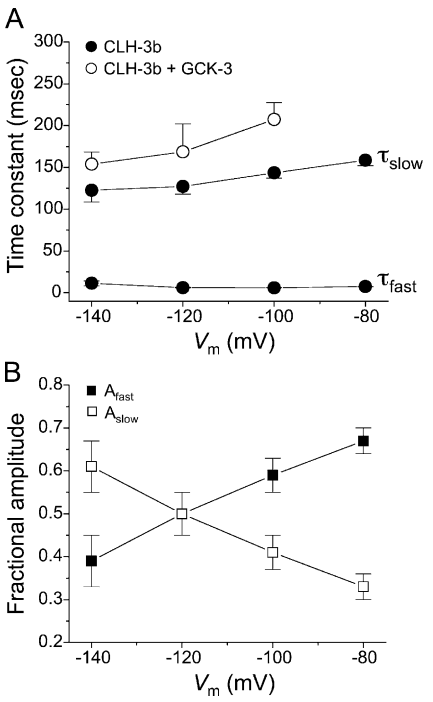

FIGURE 4. GCK-3 coexpression alters a fast gating process in CLH-3b. (A) Time constants of hyperpolarization-induced activation of CLH-3b when expressed alone or together with GCK-3. $I_{CLH\text{-}3b}$ activation in cells expressing CLH-3b alone is well described by the sum of two time constants (i.e., τ_{fast} and τ_{slow}), whereas activation of the kinase-inhibited current is described by a single time constant. (B) Relative amplitudes versus voltage of the fast and slow components, A_f and A_s, of $I_{CLH\text{-}3b}$ in cells expressing CLH-3b alone. A_f and A_s are defined as $a_f/(a_f + a_s)$ and $a_s/(a_f + a_s)$, where a_f and a_s are the amplitudes of the fast and slow components of the bi-exponential fits (Tzounopoulos et al., 1998). Values are means ± SEM (n = 7–8).

and 50% rise time from −72 to −38 mV and 172 to 26 ms, respectively (Fig. 3, C and D, bars on left).

As a final test for the role of GCK-3–mediated phosphorylation in CLH-3b regulation, we coexpressed the channel with a kinase-defective GCK-3 mutant. The catalytic domains of GCK-3 and PASK/SPAK as well as many other kinases are highly conserved (Hanks and Hunter, 1995). An essential lysine residue is required for positioning of the terminal phosphate group of ATP (Hanks and Hunter, 1995). Mutation of this lysine (K101) to arginine (K101R) in PASK/SPAK abolishes catalytic activity (Ushiro et al., 1998; Johnston et al., 2000; Dowd and Forbush, 2003). We mutated the corresponding lysine (K137; highlighted by asterisk in Fig. 1 B) to arginine (K137R). As summarized in Fig. 3 B, GCK-3(K137R) did not inhibit CLH-3b activity. $I_{CLH\text{-}3b}$ density recorded in cells coexpressing GCK-3(K137R) was 2–9-fold ($P < 0.05$) greater than that recorded in cells coexpressing wild-type GCK-3. Furthermore, GCK-3(K137R) coexpression failed to shift $I_{CLH\text{-}3b}$ activation voltage or slow the channel's activation kinetics (Fig. 3, C and D, bars on right). Taken together, these results demonstrate clearly that inhibition of CLH-3b by GCK-3 requires the kinase activity of the protein.

GCK-3 Alters a Fast Gating Process in CLH-3b

We derived time constants for hyperpolarization-induced current activation by fitting current traces with exponential functions during the first 500 ms of hyperpolarizing test pulses. In cells where CLH-3b was expressed alone, voltage-dependent $I_{CLH\text{-}3b}$ activation was well described by the sum of two exponential terms describing fast and slow time constants that differed by a factor of 10–20 (Fig. 4 A). The fractional amplitudes of the fast and slow time constants were voltage dependent (Fig. 4 B). In contrast, the GCK-3–inhibited current could be well described by a single time constant similar to the slow time constant of $I_{CLH\text{-}3b}$ in cells expressing CLH-3b alone (Fig. 4). These data suggest that activation gating in the fully active channel occurs by fast and slow processes, and that activation of the GCK-3–inhibited current is dominated by a single, slow process that is kinetically similar to the slow process observed when the channel is expressed alone.

Binding of GCK-3 to CLH-3b Is Required for Channel Inhibition

Delpire and coworkers (Piechotta et al., 2002) demonstrated that PASK/SPAK binds to cation coupled Cl^- cotransporters via the motif (R/K)FX(V/I). Mutation of the phenylalanine residue at position 2 in this motif to alanine abolishes the interaction (Piechotta et al., 2002). We identified a similar motif, RFLI, in CLH-3b beginning at arginine 678. This putative GCK-3 binding domain is located at the beginning of exon 12, which is present only in the CLH-3b splice variant (Nehrke et al., 2000; Denton et al., 2004). To test whether this motif is required for interaction of GCK-3 and CLH-3b, we mutated phenylalanine 679 to alanine (F679A) and performed yeast two-hybrid analysis using wild-type and mutant CLH-3b COOH terminus as bait.

Fig. 5 A shows β-galactosidase activity in extracts of yeast coexpressing the strongly interacting protein pair TD1 and VA3 (TD1/VA3), the CLH-3b COOH terminus and the GAL4 activation domain (CLH-3b/GAL4AD), the wild-type CLH-3b COOH terminus and the last 178 amino acids of GCK-3 ligated downstream of GAL4AD (CLH-3b/GCK-3), or the F679A CLH-3b mutant COOH terminus and the last 178 amino acids of GCK-3 ligated downstream of GAL4AD (F679A/GCK-3). Results are expressed relative to yeast expressing TD1 and VA3. β-galactosidase activity in CLH-3b/GCK-3 yeast extracts was ∼40% of that observed with TD1/VA3. The F679A mutation reduced β-galactosidase activity to a level that was not significantly ($P > 0.05$) different from background levels observed in CLH-3b/GAL4AD yeast extracts. These results demon-

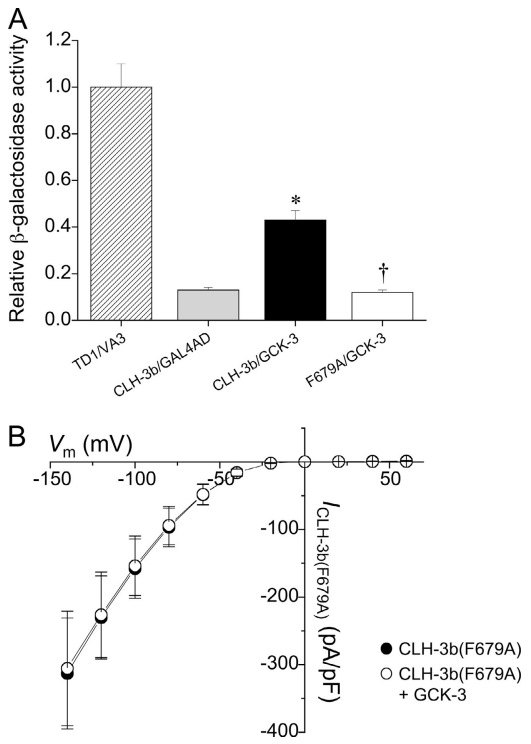

FIGURE 5. GCK-3 regulation of CLH-3b requires kinase binding to the channel COOH terminus. (A) Characterization of GCK-3/CLH-3b interaction by yeast two-hybrid assay. Interaction pairs: CLH-3b/GAL4AD, CLH-3b COOH terminus and the GAL4 activation domain; CLH-3b/GCK-3, wild-type CLH-3b COOH terminus and the last 178 amino acids of GCK-3 ligated downstream of GAL4AD; F679A/GCK-3, F679A CLH-3b mutant COOH terminus and the last 178 amino acids of GCK-3 ligated downstream of GAL4AD. β-Galactosidase activity is expressed relative to the strongly interacting protein pair TD1 and VA3 (TD1/VA3). Values are means ± SEM ($n = 3$). *, $P < 0.001$ compared with CLH-3b/GAL4AD. †, $P < 0.001$ compared with CLH-3b/GCK-3. (B) Current-to-voltage relationships of whole cell currents in cells expressing CLH-3b(F679A) mutant or CLH-3b(F679A) mutant and GCK-3. Values are means ± SEM ($n = 8$–9).

strate that the (R/K)FX(V/I) binding motif also mediates the interaction of GCK-3 with CLH-3b.

PASK/SPAK binding to the Na-K-2Cl cotransporter is not required for regulation (Dowd and Forbush, 2003). To determine whether GCK-3–mediated regulation of CLH-3b requires kinase binding to the channel, we coexpressed the CLH-3b(F679A) mutant with and without GCK-3 and characterized whole-cell Cl^- currents. As shown in Fig. 5 B, whole cell current density in cells expressing CLH-3b(F679A) alone was not significantly ($P > 0.9$) different from cells coexpressing GCK-3 and the F679A mutant. Mean ± SEM activation voltage and 50% rise time at −100 mV in cells coexpressing CLH-3b(F679A) and GCK-3 were −31 ± 0.6 mV and 5 ± 0.5 ms ($n = 8$), respectively, and were not significantly ($P > 0.05$) different from those observed in cells expressing either wild-type CLH-3b (Fig. 2 C) or CLH-3b(F679A) alone (mean ± SEM activation voltage = −31 ± 0.4 mV; mean ± SEM; 50% rise time at −100 mV = 5 ± 0.8 ms; $n = 9$). These results indicate that a physical interaction between GCK-3 and CLH-3b is required for kinase-dependent regulation of channel activity.

gck-3 and clh-3 Are Coexpressed in the Worm Oocyte and Excretory Cell

Data shown in Figs. 2–5 demonstrate clearly that GCK-3 functions to inhibit heterologously expressed CLH-3b by phosphorylating the channel and/or associated regulatory proteins. To test whether the kinase plays a physiologically relevant role in CLH-3b regulation, we first examined its expression pattern by RT-PCR and GFP transcriptional reporter methods.

GFP reporter studies have demonstrated that *clh-3* is transcriptionally expressed in the excretory cell, vulval cells, uterus, hermaphrodite-specific neurons, enteric muscles, and the first four epithelial cells of the intestine. Expression of the channel is particularly prominent in the excretory cell where it may function in regulation of whole animal salt and water balance (Schriever et al., 1999; Nehrke et al., 2000). To assess the tissue distribution of GCK-3, we generated two independent transgenic worm strains expressing a *gck-3*::GFP transcriptional reporter (termed P*gck-3*::GFP) comprised of 3.5 kb of genomic sequence 5′ to the *gck-3* start site fused to GFP. As shown in Fig. 6 A (right panel), GCK-3 is also expressed strongly in the excretory cell. No obvious GFP expression was detected in any other cell type.

Microinjected transgenes generally do not express well in *C. elegans* germ cells. To determine if GCK-3 is expressed in the worm oocyte, we used single oocyte RT-RCR. As shown in Fig. 6 A (left panel), *gck-3* transcripts of the predicted size are present in oocytes. The coexpression of *gck-3* and *clh-3* in the excretory cell and oocyte combined with results from heterologous expression studies shown in Figs. 2–4 is consistent with the idea that GCK-3 is a binding partner of CLH-3b and that it regulates channel activity in vivo.

RNAi Knockdown of GCK-3 Activity Induces Constitutive Activation of Native CLH-3b

If GCK-3 regulates CLH-3b in vivo, loss of kinase activity should induce net protein dephosphorylation and constitutive channel activation. To test this idea, we patch clamped oocytes isolated from worms microinjected with either GFP or GCK-3 double strand RNA (dsRNA). Control oocytes from GFP dsRNA–injected worms showed typical basal levels of CLH-3b current (Fig. 6 B). In contrast, current levels measured at test voltages between −40 and −100 mV in oocytes from GCK-3 RNAi worms were 4–60-fold higher ($P < 0.001$; Fig. 6 B). The activation voltage of I_{CLH-3b} in oo-

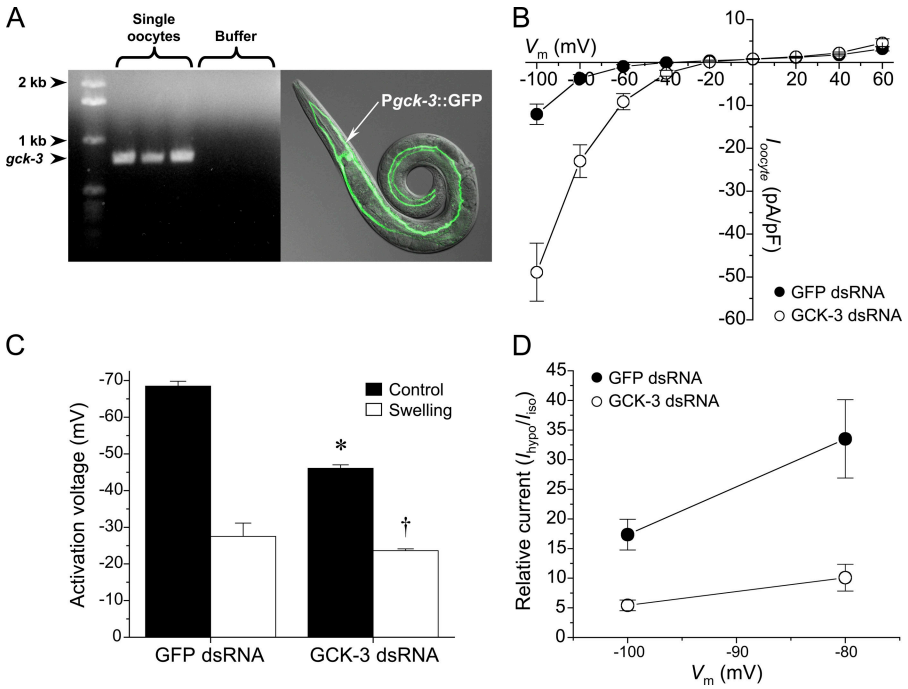

FIGURE 6. GCK-3 regulates CLH-3b activity in vivo. (A) *gck-3* and *clh-3* are co-expressed in *C. elegans* oocytes and the excretory cell. Left, detection of GCK-3 transcripts in single worm oocytes by RT-PCR. Expected product sizes of amplified GCK-3 cDNA and genomic DNA are 0.8 kb and 3.5 kb, respectively. Transcripts were not detected in samples of oocyte wash buffer. Right, combined confocal differential interference contrast and fluorescence micrographs showing expression of the *gck-3* transcriptional reporter, P*gck-3*::GFP, in the H-shaped excretory cell. This GFP expression pattern was observed in two independent lines of transgenic worms. (B) GCK-3 knockdown constitutively activates CLH-3b in meiotically arrested *C. elegans* oocytes. Whole cell currents measured in GCK-3 RNAi oocytes between −40 and −100 mV were significantly ($P < 0.004$) different form those measured in control GFP RNAi oocytes. Values are means ± SEM (n = 8–11). GFP and GCK-3 dsRNA injections were performed in parallel on two separate groups of worms. (C) CLH-3b activation voltages in oocytes isolated from GFP and GCK-3 dsRNA–injected worms. Values are means ± SEM (n = 8–11). *, $P < 0.0001$ compared with oocytes from GFP dsRNA-injected worms. †, $P < 0.0001$ compared with nonswollen GCK-3 RNAi oocytes. (D) Relative swelling-induced whole cell current in GFP or GCK-3 RNAi oocytes. Cells were swollen for 5 min. Values are means ± SEM (n = 5–6). Relative current values were calculated only for test potentials where the current amplitude was measurable.

cytes from GCK-3 RNAi animals was significantly ($P < 0.0001$) more depolarized than that in control oocytes (Fig. 6 C). Increased basal current levels and depolarized activation voltages are consistent with dephosphorylation-dependent CLH-3b activation induced by loss of GCK-3 kinase activity.

The 50% rise time for hyperpolarization-induced current activation at −100 mV was not significantly ($P > 0.05$) altered by GCK-3 knockdown (unpublished data), suggesting that disruption of *gck-3* expression only partially activated CLH-3b. Consistent with this, we observed that swelling GCK-3 RNAi oocytes for 5 min further activated $I_{CLH\text{-}3b}$ by 5–10-fold (Fig. 6 D; n = 5). In sharp contrast, swelling GFP RNAi oocytes for 5 min activated $I_{CLH\text{-}3b}$ by 17–35-fold (Fig. 6 D; n = 6). The rates of swelling-induced $I_{CLH\text{-}3b}$ activation were not significantly different ($P > 0.1$) for GFP and GCK-3 RNAi oocytes (mean ± SEM rates of $I_{CLH\text{-}3b}$ activation at −100 mV in GFP and GCK-3 RNAi oocytes were −0.74 ± 0.13 pA/pF/s and −0.47 ± 0.05 pA/pF/s; n = 5–6). Taken together, these results indicate that knockdown of GCK-3 expression partially activates CLH-3b in the oocyte. Partial channel activation may be due to incomplete knockdown of *gck-3* expression and/or the existence of other kinases with redundant functions. In yeast for example, Ste20 and the related Cla4 kinase function redundantly in certain cellular processes (e.g., Cvrckova et al., 1995; Weiss et al., 2000; Chiroli et al., 2003). Furthermore, at least two type-1 phosphatases, GLC-7α and GCL-7β, mediate dephosphorylation events that activate CLH-3b in the worm oocyte (Rutledge et al., 2002).

DISCUSSION

ClC-0, the first member of the ClC superfamily of voltage-gated anion channels, was identified in 1990 by expression cloning from the *Torpedo* electric organ (Jentsch et al., 1990). Members of this gene family have since been found in organisms ranging from bacteria to mammals (Jentsch et al., 2002). Much of our understanding of the physiological roles of ClC channels has come from knockout studies in mice and identification of disease-causing mutations in humans (Jentsch et al., 2002; Haug et al., 2003).

Little is known about how ClC channels are regulated. Phosphorylation events have been shown to modulate the activity of various ClCs, but the signaling pathways involved and the physiological context under which this regulation occurs are uncertain. For example, human ClC-1 expressed heterologously in HEK293 cells is inhibited by phorbol ester–induced activation of PKC (Rosenbohm et al., 1999). Dialysis of cells patch clamped in the whole-cell mode with autonomously active calcium/calmodulin-dependent protein kinase II (CaMKII) activates heterologously expressed human

ClC-3 (Huang et al., 2001). Guinea pig ClC-3 is inhibited by phorbol esters or cAMP in PKC and PKA-dependent manners (Duan et al., 1999; Nagasaki et al., 2000). ClC-2 expressed in *Xenopus* oocytes is inhibited by injection of activated p34cdc2/cyclin B, which also phosphorylates the channel protein in vitro and in cell-free oocyte microsome assays (Furukawa et al., 2002).

We have used the genetically tractable model organism *C. elegans* to further characterize the physiological roles of ClC channels and to define the mechanisms and signaling pathways by which they are regulated. CLH-3b is a member of the ClC-1/2/Ka/Kb subfamily and is functionally expressed in the nematode oocyte (Rutledge et al., 2001, 2002; Denton et al., 2004). In nonmaturing oocytes, CLH-3b is activated by cell swelling, but the channel appears to play no role in regulatory volume decrease (Rutledge et al., 2001).

The physiologically relevant regulator of CLH-3b activity is the oocyte meiotic cell cycle (Rutledge et al., 2001). Adult *C. elegans* hermaphrodites possess two U-shaped gonad arms connected via spermatheca to a common uterus. Oocytes form in the proximal gonad and accumulate in a single-file row of graded developmental stages. Developing oocytes remain in diakinesis of prophase I until they reach the most proximal position in the gonad arm where meiosis resumes, a process termed meiotic maturation (for review see Hubbard and Greenstein, 2000). Meiotic maturation triggers activation of CLH-3b (Rutledge et al., 2001) and induces ovulation (for review see Hubbard and Greenstein, 2000). CLH-3b plays a role in regulating ovulation by controlling the contractile activity of myoepithelial sheath cells that surround and are coupled to oocytes via gap junctions (Rutledge et al., 2001; Strange, 2002; Yin et al., 2004).

Both swelling- and meiotic maturation–induced activation of CLH-3b are mediated by serine/threonine dephosphorylation (Rutledge et al., 2002). The identification of GCK-3 as a kinase that binds to and functions to inhibit the channel is consistent with known physiological roles of the Ste20 superfamily. Ste20 kinases play important regulatory roles in cell cycle–dependent physiological processes and cellular stress responses (Dan et al., 2001). Of particular relevance for CLH-3b regulation are observations demonstrating that yeast Ste20 kinase is activated by hypertonic cell shrinkage (Raitt et al., 2000) and that X-PAK activity functions to maintain *Xenopus* oocytes in meiotic arrest (Faure et al., 1997, 1999; Cau et al., 2000). CLH-3b is inhibited in meiotic cell cycle–arrested oocytes and by oocyte shrinkage (Rutledge et al., 2001).

As shown in Fig. 4, hyperpolarization-induced activation of CLH-3b expressed alone occurs via fast and slow gating processes, whereas a single, slow process dominates voltage-dependent activation of GCK-3–inhibited channels. Fast and slow time constants have been derived from exponential fits of gating relaxations in ClC-1 and ClC-2 (Saviane et al., 1999; Bennetts et al., 2001; Zuniga et al., 2004). Fast relaxations are thought to reflect opening and closing of individual protopore gates that operate independently of one another and on a millisecond time scale. Slow relaxations have been ascribed to the function of a common gate that opens and closes both protopores simultaneously.

Structural studies on bacterial ClC homologues as well as functional studies on ClC-0 and ClC-2 suggest that a glutamate residue positioned in the extracellular opening of each protopore functions as the fast protopore gate (Dutzler et al., 2003; Niemeyer et al., 2003). With the exception of ClC-Ka and ClC-Kb, this glutamate residue is conserved in all ClC channels, including CLH-3b (Denton et al., 2004). In the absence of CLH-3b single channel measurements, we do not yet know if hyperpolarization-induced activation of CLH-3b is regulated by fast and slow gating mechanisms analogous to those of other ClCs. It is nevertheless interesting to speculate that the fast gating process in CLH-3b represents opening of the protopore gate, and that GCK-3–mediated phosphorylation inhibits this process. Interestingly, Dutzler et al. (2002) showed that the α-helix immediately preceding the intracellular COOH terminus of bacterial ClC channels is a structural component of the protopore. They speculated that the COOH terminus could therefore provide a direct route for regulating channel gating by intracellular signaling events.

The binding of GCK-3 to the COOH terminus suggests that this part of the channel could be a target of regulatory phosphorylation. If this is the case, phosphorylation-dependent changes in the structure of the COOH terminus may regulate channel activation by regulating the protopore glutamate gate. Detailed studies are currently underway to elucidate the biochemical, structural, and biophysical mechanisms underlying GCK-3–mediated inhibition of CLH-3b.

Delpire and coworkers (Piechotta et al., 2002) demonstrated that the GCK-3 homologues, PASK/SPAK and OSR1 (Fig. 1 B), bind to swelling-activated K-Cl and shrinkage-activated Na-K-2Cl cotransporters. Activation of K-Cl and Na-K-2Cl cotransporters is mediated by serine/threonine dephosphorylation and phosphorylation, respectively (Haas and Forbush, 2000; Lauf and Adragna, 2000; Russell, 2000). Compelling evidence suggests that a common volume-sensitive kinase mediates cell volume–dependent regulation of both cotransporters (Lytle, 1997, 1998; Lytle and McManus, 2002). Dowd and Forbush (2003) have shown recently that PASK/SPAK functions in shrinkage-induced activation of the Na-K-2Cl cotransporter NKCC1. These results, taken together with our findings, suggest that GCK-3

and its mammalian homologue PASK/SPAK are themselves volume-sensitive kinases or components of a volume-sensitive kinase cascade.

In many organisms and cell types, cell cycle progression is linked tightly to changes in cell volume (Potter and Xu, 2001; Saucedo and Edgar, 2002; Mitchison, 2003). Furthermore, volume-sensitive anion channels and K-Cl and Na-K-2Cl cotransporters have been implicated in the regulation of cell cycle events, cell growth and proliferation, and programmed cell death (Russell, 2000; Eggermont et al., 2001; Okada and Maeno, 2001; Shen et al., 2001, 2003). It is interesting to speculate that Ste20-type kinases may represent a common link between cell volume change and the cell cycle.

What regulatory mechanisms could mediate such a link? During development, the volume of a *C. elegans* oocyte increases ~200-fold before induction of meiotic maturation and ovulation (Hall et al., 1999; McCarter et al., 1999). Interestingly, we have observed that the sensitivity of CLH-3b to swelling is inversely related to oocyte size; channel activation requires much greater cell swelling in small, early stage oocytes compared with larger, later stage oocytes (Rutledge et al., 2001). A possible explanation for these observations is that a regulatory protein analogous to cyclins, which control cyclin-dependent kinases (Ekholm and Reed, 2000; Kishimoto, 2003), may function directly or indirectly to activate GCK-3. Like cyclins, the intracellular levels of this putative regulatory protein could vary with the cell cycle. The simplest hypothesis that would explain our observations is that the concentration of GCK-3 regulatory proteins falls as oocytes grow and develop. Cell cycle– and growth-dependent reduction of GCK-3 activity below a critical level would lead to net protein dephosphorylation and activation of CLH-3b in maturing oocytes. Inhibition of GCK-3 could also participate in the regulation of meiotic cell cycle progression as has been proposed for X-PAKs in *Xenopus* oocytes (Faure et al., 1997, 1999; Cau et al., 2000). Oocyte swelling may activate CLH-3b by artificially lowering GCK-3 regulatory protein concentration, thereby inhibiting kinase function. Further studies to address this possibility are warranted.

The regulation of both Cl^- channels and cation-coupled cotransporters by Ste20 homologues is intriguing and has important physiological implications. Coordinated regulation of Cl^- leaks (i.e., channels) and pumps (i.e., cotransporters) is essential for efficient cell volume control and transepithelial Cl^- and fluid transport. In response to shrinkage, cells accumulate NaCl and osmotically obliged water via activation of the Na-K-2Cl cotransporter (Haas and Forbush, 2000; Lauf and Adragna, 2000; Russell, 2000). Shrinkage-induced activation of the cotransporter and concomitant inhibition of Cl^- leaks by a common kinase would increase the rate of net NaCl accumulation and volume recovery.

Fluid secretion in secretory epithelia such as the salivary gland, intestine, and lung is mediated by activation of basolateral Na-K-2Cl cotransporters and apical Cl^- channels such as CFTR (Haas and Forbush, 2000). Concomitant activation of the cotransporter and inhibition of basolateral Cl^- leaks would increase net secretory Cl^- and water transport. In this regard, it is interesting to note that *gck-3* and *clh-3* are not only coexpressed in the worm oocyte, but also the worm excretory cell (Fig. 6 A; Schriever et al., 1999; Nehrke et al., 2000). The excretory cell is a secretory cell responsible for whole animal fluid excretion (Nelson et al., 1983; Nelson and Riddle, 1984). Two predicted Na-K-2Cl cotransporter encoding genes are present in the *C. elegans* genome, and both of these predicted cotransporters contain putative PASK/SPAK binding motifs. It will be interesting to determine whether Na-K-2Cl cotransporters and *clh-3* encoded channels are colocalized in the excretory cell and coordinately regulated by GCK-3 to mediate fluid secretion.

In conclusion, we have identified a novel Ste20 kinase, GCK-3, that binds to and regulates that activity of a ClC anion channel. Numerous members of several channel and transporter families contain Ste20 binding motifs (Piechotta et al., 2002), suggesting that Ste20-type kinases may play a widespread role in regulation of membrane transport processes. GCK-3–mediated serine/threonine phosphorylation functions to inhibit CLH-3b activity in meiotic cell cycle–arrested, nonswollen *C. elegans* oocytes. Our studies provide new insight into physiologically relevant signaling pathways that control ClC channel activity and suggest novel mechanisms for coupling cell volume changes to cell cycle events and for coordinately regulating ion channels and transporters that control cellular Cl^- content, cell volume, and epithelial fluid secretion.

This work was supported by National Institutes of Health (NIH) grants R01 DK61168 and DK51610 to K. Strange, by R01 HL80810 to K. Nehrke, by R01 DE09692 to J. Melvin, and by NIH National Research Service Award F32 GM067424 and NIH training grant T32 NS07491 to J. Denton. Confocal microscopy was performed in the Vanderbilt University Medical Center Cell Imaging Shared Resource, which is supported by NIH grants CA68485, DK20593, DK58404, HD15052, and EY08126.

Angus C. Nairn served as editor.

Submitted: 12 November 2004
Accepted: 6 January 2005

REFERENCES

Bennetts, B., M.L. Roberts, A.H. Bretag, and G.Y. Rychkov. 2001. Temperature dependence of human muscle ClC-1 chloride channel. *J. Physiol.* 535:83–93.

Brenner, S. 1974. The genetics of *Caenorhabditis elegans*. *Genetics*. 77: 71–94.

Cau, J., S. Faure, S. Vigneron, J.C. Labbe, C. Delsert, and N. Morin. 2000. Regulation of *Xenopus* p21-activated kinase (X-PAK2) by

Cdc42 and maturation-promoting factor controls *Xenopus* oocyte maturation. *J. Biol. Chem.* 275:2367–2375.

Chiroli, E., R. Fraschini, A. Beretta, M. Tonelli, G. Lucchini, and S. Piatti. 2003. Budding yeast PAK kinases regulate mitotic exit by two different mechanisms. *J. Cell Biol.* 160:857–874.

Cvrckova, F., C. DeVirgilio, E. Manser, J.R. Pringle, and K. Nasmyth. 1995. Ste20-like protein kinases are required for normal localization of cell growth and for cytokinesis in budding yeast. *Genes Dev.* 9:1817–1830.

Dan, I., N.M. Watanabe, and A. Kusumi. 2001. The Ste20 group kinases as regulators of MAP kinase cascades. *Trends Cell Biol.* 11: 220–230.

Denton, J., K. Nehrke, E. Rutledge, R. Morrison, and K. Strange. 2004. Alternative splicing of N- and C-termini of a *C. elegans* ClC channel alters gating and sensitivity to external Cl^- and H^+. *J. Physiol.* 555:97–114.

Dowd, B.F., and B. Forbush. 2003. PASK (proline-alanine-rich STE20-related kinase), a regulatory kinase of the Na-K-Cl cotransporter (NKCC1). *J. Biol. Chem.* 278:27347–27353.

Duan, D., S. Cowley, B. Horowitz, and J.R. Hume. 1999. A serine residue in ClC-3 links phosphorylation-dephosphorylation to chloride channel regulation by cell volume. *J. Gen. Physiol.* 113: 57–70.

Dutzler, R., E.B. Campbell, M. Cadene, B.T. Chait, and R. MacKinnon. 2002. X-ray structure of a ClC chloride channel at 3.0 A reveals the molecular basis of anion selectivity. *Nature.* 415:287–294.

Dutzler, R., E.B. Campbell, and R. MacKinnon. 2003. Gating the selectivity filter in ClC chloride channels. *Science.* 300:108–112.

Eggermont, J., D. Trouet, I. Carton, and B. Nilius. 2001. Cellular function and control of volume-regulated anion channels. *Cell Biochem. Biophys.* 35:263–274.

Ekholm, S.V., and S.I. Reed. 2000. Regulation of G_1 cyclin-dependent kinases in the mammalian cell cycle. *Curr. Opin. Cell Biol.* 12: 676–684.

Elion, E.A. 2000. Pheromone response, mating and cell biology. *Curr. Opin. Microbiol.* 3:573–581.

Faure, S., S. Vigneron, M. Doree, and N. Morin. 1997. A member of the Ste20/PAK family of protein kinases is involved in both arrest of *Xenopus* oocytes at G2/prophase of the first meiotic cell cycle and in prevention of apoptosis. *EMBO J.* 16:5550–5561.

Faure, S., S. Vigneron, S. Galas, T. Brassac, C. Delsert, and N. Morin. 1999. Control of G2/M transition in *Xenopus* by a member of the p21-activated kinase (PAK) family: a link between protein kinase A and PAK signaling pathways? *J. Biol. Chem.* 274: 3573–3579.

Furukawa, T., T. Ogura, Y.-J. Zheng, H. Tsuchiya, H. Nakaya, Y. Katayama, and N. Inagaki. 2002. Phosphorylation and functional regulation of ClC-2 chloride channels expressed in *Xenopus* oocytes by M cyclin-dependent protein kinase. *J. Physiol.* 540:883–893.

Haas, M., and B. Forbush. 2000. The Na-K-Cl cotransporter of secretory epithelia. *Annu. Rev. Physiol.* 62:515–534.

Hall, D.H., V.P. Winfrey, G. Blaeuer, L.H. Hoffman, T. Furuta, K.L. Rose, O. Hobert, and D. Greenstein. 1999. Ultrastructural features of the adult hermaphrodite gonad of *Caenorhabditis elegans*: relations between the germ line and soma. *Dev. Biol.* 212:101–123.

Hanks, S.K., and T. Hunter. 1995. Protein kinases 6. The eukaryotic protein kinase superfamily: kinase (catalytic) domain structure and classification. *FASEB J.* 9:576–596.

Haug, K., M. Warnstedt, A.K. Alekov, T. Sander, A. Ramirez, B. Poser, S. Maljevic, S. Hebeisen, C. Kubisch, J. Rebstock, et al. 2003. Mutations in CLCN2 encoding a voltage-gated chloride channel are associated with idiopathic generalized epilepsies. *Nat. Genet.* 33:527–532.

Huang, P., J. Liu, A. Di, N.C. Robinson, M.W. Musch, M.A. Kaetzel, and D.J. Nelson. 2001. Regulation of human CLC-3 channels by multifunctional Ca^{2+}/calmodulin-dependent protein kinase. *J. Biol. Chem.* 276:20093–20100.

Hubbard, E.J., and D. Greenstein. 2000. The *Caenorhabditis elegans* gonad: a test tube for cell and developmental biology. *Dev. Dyn.* 218:2–22.

Jentsch, T.J., K. Steinmeyer, and G. Schwarz. 1990. Primary structure of *Torpedo marmorata* chloride channel isolated by expression cloning in *Xenopus* oocytes. *Nature.* 348:510–514.

Jentsch, T.J., V. Stein, F. Weinreich, and A.A. Zdebik. 2002. Molecular structure and physiological function of chloride channels. *Physiol. Rev.* 82:503–568.

Johnston, A.M., G. Naselli, L.J. Gonez, R.M. Martin, L.C. Harrison, and H.J. Deaizpurua. 2000. SPAK, a STE20/SPS1-related kinase that activates the p38 pathway. *Oncogene.* 19:4290–4297.

Kishimoto, T. 2003. Cell-cycle control during meiotic maturation. *Curr. Opin. Cell Biol.* 15:654–663.

Lauf, P.K., and N.C. Adragna. 2000. K-Cl cotransport: properties and molecular mechanism. *Cell. Physiol. Biochem.* 10:341–354.

Lytle, C. 1997. Activation of the avian erythrocyte Na-K-Cl cotransport protein by cell shrinkage, cAMP, fluoride, and calyculin-A involves phosphorylation at common sites. *J. Biol. Chem.* 272: 15069–15077.

Lytle, C. 1998. A volume-sensitive protein kinase regulates the Na-K-2Cl cotransporter in duck red blood cells. *Am. J. Physiol.* 274: C1002–C1010.

Lytle, C., and T. McManus. 2002. Coordinate modulation of Na-K-2Cl cotransport and K-Cl cotransport by cell volume and chloride. *Am. J. Physiol. Cell Physiol.* 283:C1422–C1431.

McCarter, J., B. Bartlett, T. Dang, and T. Schedl. 1999. On the control of oocyte meiotic maturation and ovulation in *Caenorhabditis elegans*. *Dev. Biol.* 205:111–128.

Mello, C.C., J.M. Kramer, D. Stinchcomb, and V. Ambros. 1991. Efficient gene transfer in *C. elegans*: extrachromosomal maintenance and integration of transforming sequences. *EMBO J.* 10: 3959–3970.

Mitchison, J.M. 2003. Growth during the cell cycle. *Int. Rev. Cytol.* 226:165–258.

Nagasaki, M., L. Ye, D. Duan, B. Horowitz, and J.R. Hume. 2000. Intracellular cyclic AMP inhibits native and recombinant volume-regulated chloride channels from mammalian heart. *J. Physiol.* 523(Pt 3):705–717.

Nehrke, K., and J.E. Melvin. 2002. The NHX family of Na^+-H^+ exchangers in *Caenorhabditis elegans*. *J. Biol. Chem.* 277:29036–29044.

Nehrke, K., T. Begenisich, J. Pilato, and J.E. Melvin. 2000. Into ion channel and transporter function. *C. elegans* ClC-type chloride channels: novel variants and functional expression. *Am. J. Physiol. Cell Physiol.* 279:C2052–C2066.

Nelson, F.K., and D.L. Riddle. 1984. Functional study of the *Caenorhabditis elegans* secretory-excretory system using laser microsurgery. *J. Exp. Zool.* 231:45–56.

Nelson, F.K., P.S. Albert, and D.L. Riddle. 1983. Fine structure of the *Caenorhabditis elegans* secretory-excretory system. *J. Ultrastruct. Res.* 82:156–171.

Niemeyer, M.I., L.P. Cid, L. Zuniga, M. Catalan, and F.V. Sepulveda. 2003. A conserved pore-lining glutamate as a voltage- and chloride-dependent gate in the ClC-2 chloride channel. *J. Physiol.* 553:873–879.

Okada, Y., and E. Maeno. 2001. Apoptosis, cell volume regulation and volume-regulatory chloride channels. *Comp. Biochem. Physiol. A Mol. Integr. Physiol.* 130:377–383.

Piechotta, K., J. Lu, and E. Delpire. 2002. Cation chloride cotransporters interact with the stress-related kinases Ste20-related proline-alanine-rich kinase (SPAK) and oxidative stress response 1 (OSR1). *J. Biol. Chem.* 277:50812–50819.

Potter, C.J., and T. Xu. 2001. Mechanisms of size control. *Curr. Opin. Genet. Dev.* 11:279–286.

Raitt, D.C., F. Posas, and H. Saito. 2000. Yeast Cdc42 GTPase and Ste20 PAK-like kinase regulate Sho1-dependent activation of the Hog1 MAPK pathway. *EMBO J.* 19:4623–4631.

Ramezani-Rad, M. 2003. The role of adaptor protein Ste50-dependent regulation of the MAPKKK Ste11 in multiple signalling pathways of yeast. *Curr. Genet.* 43:161–170.

Rosenbohm, A., R. Rudel, and C. Fahlke. 1999. Regulation of the human skeletal muscle chloride channel hClC-1 by protein kinase C. *J. Physiol.* 514(Pt 3):677–685.

Russell, J.M. 2000. Sodium-potassium-chloride cotransport. *Physiol. Rev.* 80:211–276.

Rutledge, E., L. Bianchi, M. Christensen, C. Boehmer, R. Morrison, A. Broslat, A.M. Beld, A. George, D. Greenstein, and K. Strange. 2001. CLH-3, a ClC-2 anion channel ortholog activated during meiotic maturation in *C. elegans* oocytes. *Curr. Biol.* 11:161–170.

Rutledge, E., J. Denton, and K. Strange. 2002. Cell cycle- and swelling-induced activation of a *C. elegans* ClC channel is mediated by CeGLC-7α/β phosphatases. *J. Cell Biol.* 158:435–444.

Saucedo, L.J., and B.A. Edgar. 2002. Why size matters: altering cell size. *Curr. Opin. Genet. Dev.* 12:565–571.

Saviane, C., F. Conti, and M. Pusch. 1999. The muscle chloride channel ClC-1 has a double-barreled appearance that is differentially affected in dominant and recessive myotonia. *J. Gen. Physiol.* 113:457–468.

Schriever, A.M., T. Friedrich, M. Pusch, and T.J. Jentsch. 1999. CLC chloride channels in *Caenorhabditis elegans*. *J. Biol. Chem.* 274: 34238–34244.

Shen, M.R., C.Y. Chou, K.F. Hsu, H.S. Liu, P.B. Dunham, E.J. Holtzman, and J.C. Ellory. 2001. The KCl cotransporter isoform KCC3 can play an important role in cell growth regulation. *Proc. Natl. Acad. Sci. USA.* 98:14714–14719.

Shen, M.R., C.Y. Chou, K.F. Hsu, Y.M. Hsu, W.T. Chiu, M.J. Tang, S.L. Alper, and J.C. Ellory. 2003. KCl cotransport is an important modulator of human cervical cancer growth and invasion. *J. Biol. Chem.* 278:39941–39950.

Strange, K. 2002. Of mice and worms: novel insights into ClC-2 anion channel physiology. *News Physiol. Sci.* 17:11–16.

Strange, K. 2003. From genes to integrative physiology: ion channel and transporter biology in *Caenorhabditis elegans*. *Physiol. Rev.* 83: 377–415.

Tzounopoulos, T., J. Maylie, and J.P. Adelman. 1998. Gating of I_{sK} channels expressed in *Xenopus* oocytes. *Biophys. J.* 74:2299–2305.

Ushiro, H., T. Tsutsumi, K. Suzuki, T. Kayahara, and K. Nakano. 1998. Molecular cloning and characterization of a novel Ste20-related protein kinase enriched in neurons and transporting epithelia. *Arch. Biochem. Biophys.* 355:233–240.

Weiss, E.L., A.C. Bishop, K.M. Shokat, and D.G. Drubin. 2000. Chemical genetic analysis of the budding-yeast p21-activated kinase Cla4p. *Nat. Cell Biol.* 2:677–685.

Yin, X., N.J. Gower, H.A. Baylis, and K. Strange. 2004. Inositol 1,4,5-trisphosphate signaling regulates rhythmic contractile activity of smooth muscle-like sheath cells in the nematode *Caenorhabditis elegans*. *Mol. Biol. Cell.* 15:3938–3949.

Zuniga, L., M.I. Niemeyer, D. Varela, M. Catalan, L.P. Cid, and F.V. Sepulveda. 2004. The voltage-dependent ClC-2 chloride channel has a dual gating mechanism. *J. Physiol.* 555:671–682.